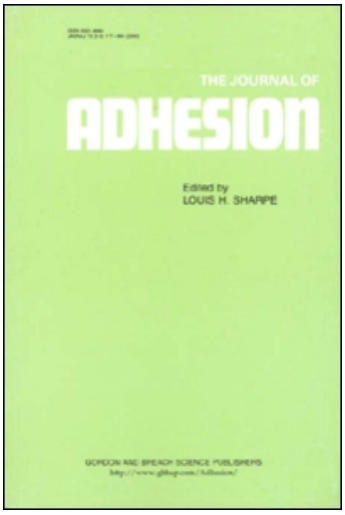

The Journal of Adhesion
Publication details, including instructions for authors and subscription information:
http://www.informaworld.com/smpp/title~content=t713453635

Adhesive Failure of Epoxy-Titanium Bonds in Aqueous Environments

E. H. Andrews; A. Stevenson[a]
[a] Department of Materials, Queen Mary College, London, England

To cite this Article Andrews, E. H. and Stevenson, A.(1980) 'Adhesive Failure of Epoxy-Titanium Bonds in Aqueous Environments', The Journal of Adhesion, 11: 1, 17 — 40
To link to this Article: DOI: 10.1080/00218468008078902
URL: http://dx.doi.org/10.1080/00218468008078902

J. Adhesion, 1980, Vol. 11, pp. 17–40
0021–8464/80/1101–0017 $04.50/0

Printed in Great Britain

Adhesive Failure of Epoxy–Titanium Bonds in Aqueous Environments

E. H. ANDREWS and A. STEVENSON

Department of Materials, Queen Mary College, London E1, England

(*Received November 5, 1979; in final form November 29, 1979*)

Plane-strain adhesive failure tests have been conducted on adhesive joints established between an epoxy resin and untreated titanium metal. The tests were carried out both before and after immersion of the specimens in water, at different temperatures and pH values as well as for different times.

Using a suitable mathematical analysis, these data provide the cohesive or adhesive failure energy of the system as a function of crack propagation speed. Generalized fracture mechanics theory can then be used to separate the contributions to the total failure energy arising from mechanical hysteresis and interfacial energy respectively. It is found that the interfacial binding energy, θ_0, decreases with the time of immersion according to a first-order chemical reaction with a rate constant which increases with the hydrogen ion concentration. The initial (dry) binding energy is approximately ten times the Van der Waals interaction energy but decreases after long times of immersion to a value about equal to this interaction energy. A probable mechanism is the acid hydrolysis of ether linkages between the epoxy resin and the titanium oxide surface.

INTRODUCTION

The deterioration of adhesive joint strength in wet environments is a problem of some importance in the engineering applications of structural adhesives. A joint which shows a high "dry strength" in the laboratory may fail at much lower stress after prolonged exposure to moisture. Warm, wet, tropical climates have proved especially damaging in this respect. This problem is at present a major obstacle to a more extensive use of adhesives in critical engineering situations and has stimulated considerable interest in the artificial ageing of adhesive joints.

The present work investigates the effect of several different environmental

factors (exposure time, temperature, environmental pH) upon the subsequent fracture resistance of a model adhesive joint. The system chosen for study is a commercial epoxy resin adhesive, bonded to an industrial grade of titanium. Fracture resistance was characterised by means of a recently introduced fracture test[1] in which an unequivocal plane strain value of fracture energy is determined as a function of crack velocity for an unstable crack.

EXPERIMENTAL METHOD

The testpiece geometry (shown in Figure 1) consisted of a cylindrical base block of titanium, E, on to which is cast a cylinder of epoxy resin, F. This arrangement has been described in detail in an earlier paper.[1] A flat circular "flaw" (B in Figure 1) is created at the epoxy/titanium interface by means of an embedded circular disc of PTFE, 250 μm in thickness. The flaw tip geometry is therefore that of a standard blunt flaw with a tip radius of 125 μm. The titanium adherend block contains a central orifice D, through which hydraulic pressure can be applied to the flaw until crack growth occurs.

Prior to casting, the titanium surfaces were simply polished to a mirror finish with a standard metal polishing wheel and cleaned by immersion in several successive baths of acetone. The epoxy resin mix was cast on to the titanium adherends within 15 minutes of their removal from the final cleansing bath, to minimise atmospheric surface contamination.

After casting, the joint was left to cure at room temperature for 24 hours and then subjected to a postcure cycle at 130°C for 1½ hours. This optimises the crosslink formation in the epoxy resin.

After postcuring, the testpieces were environmentally aged by immersion in a water bath. Each sample was totally immersed to enable water to be in contact both with the flaw tip (through the orifice) and with the external

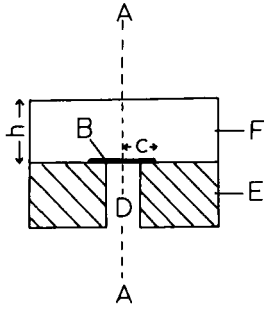

FIGURE 1 Test piece geometry, with circular symmetry about A–A. B, disc of PTFE of radius c; D, central orifice; E, base block of titanium metal; F, cast epoxy resin of height h.

edges of the interface. The temperature was held constant to within $\pm 1°C$ by sealing the environmental bath in a thermostatically controlled, airtight oven. Only the longest exposures (> 1 month) required any topping up of the environmental fluid.

All of the environmental exposures referred to here involved immersion in liquid; humid gaseous atmospheres were not used. After completion of the exposure period, the water bath was cooled slowly to room temperature when the samples were removed and dried for 24 hours in air prior to testing. Neither the duration nor the temperature of this post-exposure drying phase was found to have any effect on the subsequent joint strength. This suggests that healing of a joint weakened by water exposure does not occur.

The specimens were tested by means of a standard brittle fracture test, which involved mounting the testpiece in a specially designed hydraulic apparatus and increasing the pressure applied to the flaw until brittle fracture occurred. The maximum pressure at fracture was recorded on a UV recorder, and the crack velocity measured with the aid of high speed cinematography. The details of the test technique were described previously.[1] All tests were carried out at approximately 30°C. Subsidiary tests showed that the results are insensitive to temperature in the range $-40°C$ to 60°C.[2]

The adhesive used in all these investigations was a diglycidyl ether of bisphenol A (Shell Epikote 828) cured by mixing with a stoichiometric amount of amine hardener (Shell Epikure 114). The glass transition temperature of the cured resin was 72°C. The metal adherends were machined from rods of commercially pure titanium supplied, cleaned and annealed by Titanium International Ltd., as Ti-2. The actual composition of the titanium was: 99.4% Ti:0.03% N:0.1% C:0.01% H:0.2% Fe:0.25% 0.

FRACTURE MECHANICS ANALYSIS

The analysis appropriate to the testpiece geometry used here has been derived in detail in the earlier publication.[1] This analysis, based on linear elastic fracture mechanics, gives the following formula for the fracture energy:

$$2\mathscr{T} = P_c^2 c / E[f_1(h/c)]$$

where

$$f_1(h/c) = \frac{1}{1-\nu^2}\left\{\frac{3}{32}\left[(c/h)^3 + (c/h)\frac{4}{1-\nu}\right] + \frac{1}{\pi}\right\}^{-1} \quad (1)$$

$\mathscr{T}$ = energy required to create unit area of new crack surface (formally equal to half the critical energy release rate $\mathscr{G}_c$)

E = Youngs modulus of the resin

ν = Poisson's ratio of the resin
c = flaw radius
h = thickness of resin above flaw plane
P_c = critical pressure at fracture

The quantity $2\mathscr{T}$, will henceforth be referred to as the "cohesive fracture energy" and is related to the "intrinsic fracture energy" $\mathscr{T}_0$ by the formula[3]

$$\mathscr{T} = \mathscr{T}_0 \Phi_c \tag{2}$$

where Φ_c is a velocity and temperature dependent function describing the loss mechanisms in the bulk solid and $\mathscr{T}_0$ is analogous to γ, the surface free energy.

Equation 1 applies to the case of an embedded crack propagating through the adhesive bulk as illustrated by Figure 2 (a). When the crack propagates, instead, along the adhesive/adherend interface the elastic energy stored in the vicinity of the crack tip ("near field") is modified by the proximity of the rigid substrate surface. This leads to the following expression for the "interfacial failure energy", θ

$$\theta = \tfrac{2}{c} c/E[f_2(h/c)]$$

where

$$f_2(h/c) = \frac{1}{(1-\nu^2)}\left\{\frac{3}{32}\left[\left(\frac{c}{h}\right)^3 + \left(\frac{c}{h}\right)\frac{4}{(1-\nu)}\right] + \frac{2}{\pi}\right\}^{-1} \tag{3}$$

θ = energy required for unit area of separation of the adhesive/adherend interface.

θ is related to the true interfacial energy θ_0 by

$$\theta = \theta_0 \Phi_i \tag{4}$$

where Φ_i is a velocity and temperature dependent function describing the loss mechanisms at the interface.

These quantities $2\mathscr{T}$ and θ have been defined and discussed at greater length elsewhere [4–6].

Equations (1) and (3) lead naturally to the following energy criteria for the locus of failure:

$\theta > 2\mathscr{T}$: cohesive fracture [coh]
$\theta \sim 2\mathscr{T}$: mixed interfacial and cohesive failure [coh/adh] or [adh/coh]
$\theta < 2\mathscr{T}$: interfacial failure [adh]

In mixed mode failures, the fraction of interfacial failure will lie between 0 and 1. The expression for $2\mathscr{T}$ was used for those cases exhibiting mainly cohesive mode failure (as in Figures 2 (a) and 2 (b)), θ being used when failure was mainly interfacial (as in Figures 2 (c) and 2 (d)).

At a given temperature, each adhesive joint is thus characterised by either a $2\mathscr{T}$ vs $\dot{c}$ curve or a θ vs $\dot{c}$ curve, (where $\dot{c}$ is the velocity of the crack), the

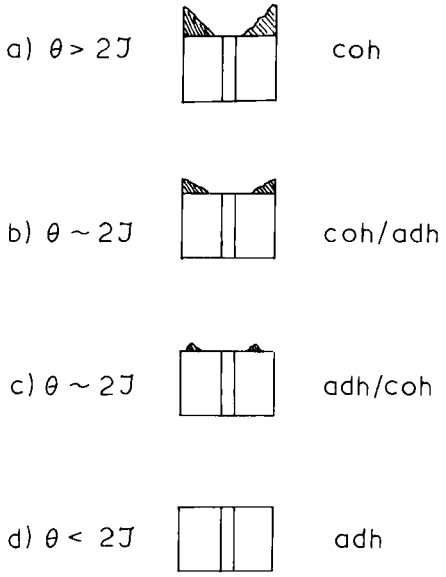

FIGURE 2 Modes of failure, with presumed relationship between θ and $2\mathscr{T}$, and "shorthand" notation. Residual resin shown shaded.

exact form of which will be determined by the loss mechanism operative (*e.g.* local plastic flow).

RESULTS

Specimens not subject to environmental exposure

Titanium/epoxy joints not subjected to environmental ageing were always found to fail in cohesive mode [coh]. The results of additional tests with brass and gold substrates were found to be indistinguishable from the result with titanium whenever cohesive mode failure [coh] occurred. This is to be expected since, with this mode of failure, $\theta > 2\mathscr{T}$ and the fracture behaviour is governed by the cohesive properties of epoxy resin. All data points from such tests conformed to the curve shown in Figure 3. It should be noted that this curve is obtained when the artificial flaw is located at the interface and differs slightly from the curve given in reference 1 where the flaw was elevated into the bulk of the resin.

Effect of exposure duration

To investigate the effect of the duration of environmental exposure on adhesive joint strength, a water environment of pH 7.8 at 80°C was adopted

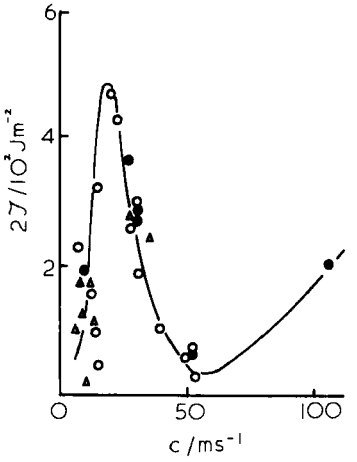

FIGURE 3 Cohesive failure energy, $2\mathcal{J}$, versus crack velocity for various metal substrates (○) titanium, (●) gold (△) brass.

as standard. Different series of testpieces were then exposed for periods ranging between 1½ hours and 120 hours. The resulting fracture behaviour is represented in Figure 4.

Specimens tested after 1½ hours exposure showed dominantly cohesive fracture [coh/adh] and conformed to the dry cohesive $2\mathcal{J}$ ($\dot{c}$) curve. After exposure of 30 hours duration the failure mode was [adh/coh], (see Figure

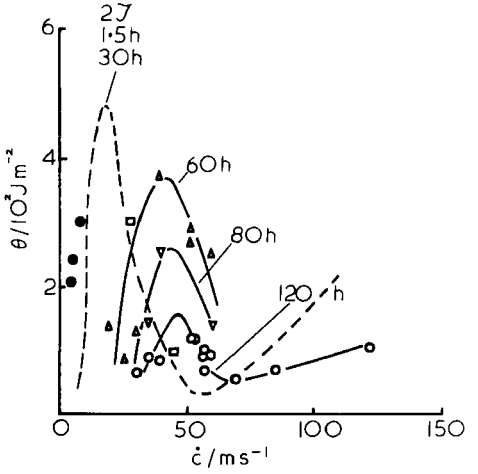

FIGURE 4 Adhesive failure energies versus crack velocity for epoxy–titanium joints after various times of immersion in water at 80°C and pH 7.8. Curve of $2\mathcal{J}$ from Figure 3 shown by broken line.

2 (c)), although the failure energies were still close to the dry $2\mathscr{T}$ ($\dot{c}$). Any toughening of the bulk may be insignificant at such short times in spite of the obvious effect of the water on the locus of failure.

Samples exposed for 60 hours exhibited a completely interfacial failure locus and a reduction in the failure energy at nearly all crack velocities. The position of θ_{max} shifts to higher crack velocity but thereafter remains approximately constant.

The overall reduction in failure energy (and hence of θ_{max}) continues as the exposure times are further increased to 80 and 120 hours.

Water may reach the interface by a process of diffusion, either through the epoxy resin bulk or along the "interphase" region between the bulk Ti and epoxy phases. The progressive change in failure locus shown in Figure 2 demonstrates that water penetration occurs simultaneously from the outer and inner boundaries. The failure locus is more sensitive to penetration from the inner boundary (via the central orifice), since crack initiation occurs here. While the extent of water penetration is small, the locus takes the form shown in Figure 2 (b), *i.e.* of a thin band of interfacial failure followed by cohesive fracturing.

When penetration from both inner and outer boundaries is substantial, the crack may return to the interface after a region of cohesive fracturing. This results in a concentric ridge of epoxy remaining on the substrate surface as illustrated in Figure 2 (c). In this case there is thus a thin central band of interface where critical water penetration has not occurred.

When the water penetration from each direction overlaps, the central ridge is eliminated as in Figure 2 (d). Prior to the onset of completely interfacial failure however there is a situation (after 80 hours immersion at 80°C on Figure 4) where irregular lumps of epoxy remain on the titanium surface. This phase is often also associated with visible internal cohesive cracking around a central concentric circle. Finally (after 120 hours) the locus of failure becomes completely interfacial, at which stage critical water penetration is clearly complete.

The rôle of water diffusion

Since the distance, Δx, of water penetration, is not always uniform on a given specimen, the *area* of adhesive failure has been used, instead, to characterize the extent of penetration. If A_1, A_2, A_3 are the annular areas respectively of interfacial failure at the exterior of the interface, of cohesive failure, and of interfacial failure around the central orifice, it is easy to show that the total area fraction of interfacial failure is

$$f_A \equiv \frac{A_1 + A_3}{A_1 + A_2 + A_3} = \frac{2\Delta x}{R} \tag{5}$$

provided the central orifice is of negligible size. R is the external radius of the specimen and the penetration distance Δx is assumed to be the same for both the outer and inner interfacial annuli. Figure 5 is a plot of f_A against $t^{\frac{1}{2}}$, where t is the time of immersion, showing excellent linearity.

The penetration of water into an epoxy resin above its glass transition temperature cannot be assumed to be Fickian, although because the amount of absorbed water is less than 10%, it may well approximate to ideal behaviour. A general equation for the penetration of a swelling agent into a polymer has been derived[7,8] having the form,

$$\Delta x = k_1 t + k_2 t^{\frac{1}{2}}$$

where Δx is the penetration depth of a sharp (non-Fickian) boundary, t is the time and k_1 and k_2 are constants.

Although this equation was derived on non-Fickian assumptions it reproduces, for $k_1 = 0$, the Fickian situation in which,[15]

$$\Delta x = 2(Dt)^{\frac{1}{2}}\text{erfc}^{-1}(C/C_0) \tag{6}$$

where D is the diffusion coefficient, C is the concentration at a penetration of Δx and C_0 is the boundary concentration. Thus Fickian behaviour is implied by the plot in Figure 5.

The relationship between Δx for interfacial failure and time is, from Eq. (6), controlled not only by the diffusion coefficient but also by the water concentration C^* required to produce interfacial failure.

If:

$$C^*/C_0 \sim 1 \quad \text{then} \quad \Delta x \ll 2(Dt)^{\frac{1}{2}}$$
$$C^*/C_0 \ll 1 \quad \text{then} \quad \Delta x \sim 2(Dt)^{\frac{1}{2}}$$

It is not therefore possible to derive a value for D from Figure 5, simply because C^* is unknown. Indeed it is not known whether a critical concentration as such exists, or whether interfacial failure is induced by a combination of water concentration and time of action. If it be assumed, however,

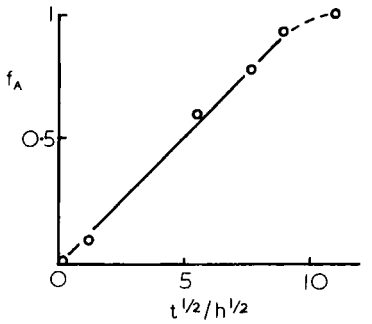

FIGURE 5 Fractional area of interfacial failure versus square root of time.

that the idea of a critical concentration is valid, then a lower limit to the value of the diffusion coefficient can be obtained for the condition $C^*/C_0 \ll 1$. In this case $D = \frac{1}{4}k_2^2$ and is of the order of $1.4 \times 10^{-11} m^2/s$. This is close to the value of $0.6 \times 10^{-11} m/s$ obtained by Gledhill, Kinloch and Shaw[9] from water uptake measurements above T_g in a similar epoxy resin. It thus appears that the progress of interfacial failure with time in the system tested is compatible with the Fickian diffusion of water through the resin to achieve a relatively low critical concentration at the interface ($C^*/C_0 \ll 1$). It is not possible, however, to rule out the possibility of a faster interfacial diffusion process associated with a high diffusion coefficient and a higher critical concentration ($C^*/C_0 \sim 1$). Clearly such a process would be limited by the self diffusion coefficient of water at around $10^{-9} m^2/s$.

Effect of environment temperature

Testpieces exposed to water of pH 7.8 for 120 hours at different temperatures, resulted in the fracture behaviour illustrated in Figure 6. Joints exposed at 20°C failed cohesively, [coh], with only a very narrow strip ($\sim 1\%$ total area) of interfacial failure around the flaw periphery. The maximum in the $2\mathcal{T}$ ($\dot{c}$) curve is however shifted to substantially higher crack velocities ($\dot{c} = 45$ m/s) and there is an elevation in $2\mathcal{T}_{max}$ compared with the behaviour of dry joints (shown in Figure 6 as a dotted line for comparison). Both of these effects probably arise from modification of the cohesive properties of the resin by the diffusion of water into its bulk. Water is thought to have a toughening effect due to plasticisation.

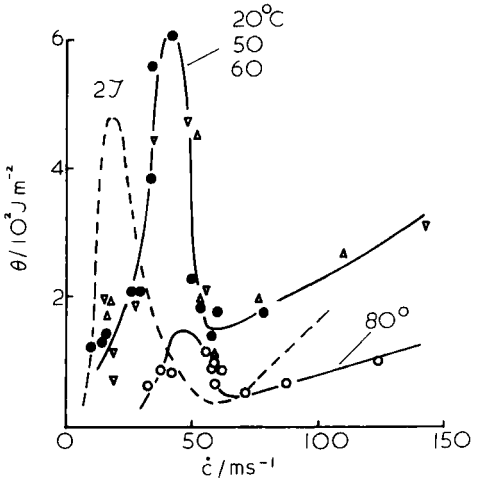

FIGURE 6 As Figure 4, but for 120 h immersion at various temperatures.

After exposure at 50°C, the fraction of interfacial failure increased to 10% (average of 15 samples), although the failure locus was still predominantly cohesive, [coh/adh], and the fracture behaviour was indistinguishable from that of specimens exposed at 20°C. The proportion of interfacial failure increased further when the exposure temperature was raised 60°C, the locus of failure now being 47% interfacial. The transition from cohesive to interfacial mode failure is illustrated in Figure 2. After exposure at 60°C the region of cohesive fracturing appears as an irregular ridge concentric with the flaw (see Figure 2 (c)). In this case the crack velocity was measured over the interfacial failure region, since the failure locus mainly followed the interface, the symbol [adh/coh] being used to refer to this type of failure.

It is difficult to distinguish between the fracture energies of testpieces after 20, 50 and 60°C exposures, when the failure locus was either [coh], [coh/adh] or [adh/coh]. On Figure 6 a single curve has therefore been drawn through all three sets of data. This curve thus represents the fracture behaviour when any significant degree of cohesive fracturing occurs.

When the exposure temperature was further increased to 80°C, the mode of failure became completely interfacial [adh] and occurred at substantially lower energies, as depicted by the lowest curve on Figure 6. The rate of diffusion may be characterised by an Arrhenius relation of the form:

$$r = A \exp(-U/RT) \tag{7}$$

where A is a constant, U is the activation energy, R is the gas constant and T is the absolute temperature. A plot of $\ln r$ versus $1/T$ would then yield a straight line. In the present case the area fraction of interfacial failure has been used to characterise the extent or rate of diffusion, and $\ln f_A$ does in fact plot linearly against reciprocal temperature, as Figure 7 shows. This plot yields a value of 80 kJ/mol for the activation energy of the diffusion of water through epoxy resin. This value is consistent with values obtained by Mason and Chiu[10]

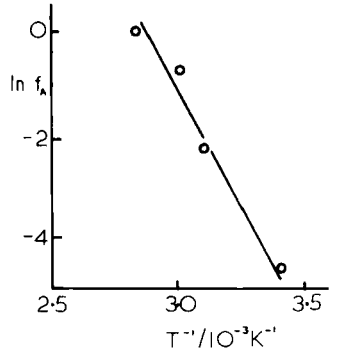

FIGURE 7 Fractional area of interfacial failure plotted logarithmically against reciprocal temperature of immersion.

who measured the weight increase of thin epoxy films exposed to water above T_g, and with values obtained by Gledhill and Kinloch[11] from similar measurements of interfacial failure in epoxy/steel and epoxy/aluminium joints after water immersion (32 kJ/mol below T_g rising to $\sim$130 kJ/mol above T_g).

The glass transition temperature of the epoxy resin used here was 72°C. The range of temperatures over which the transition from cohesive to interfacial failure was observed thus included the glass transition temperature. Substantial weakening of the interface, after exposures of reasonably short duration ($\sim$5 days), only occurred at exposure temperatures above T_g. There was no indication in our results of a transition in activation energy at T_g such as that observed by Gledhill and Kinloch using steel substrates.

The fact that the transition in locus of failure, from cohesive to interfacial, does not coincide with the reduction in failure energies (the latter only occurring after failure becomes completely interfacial) is interesting and somewhat surprising. The reason for this is not clear, but obviously the cohesive properties of the epoxy resin continue to determine failure behaviour even when a substantial proportion of interfacial failure occurs.

It is also significant that both the maximum and the minimum in the fracture energy curve occur at the same crack velocities (40 m/s and 60 m/s respectively) regardless of the locus of failure and even when failure is completely interfacial. This again highlights the importance of the rheological properties of the bulk resin even for completely interfacial modes of failure.

Effect of environment pH

The previous experiment was repeated with water of reduced hydrogen ion concentration (pH 8.6), and a considerable reduction in the weakening effect was observed. This is depicted in Figure 8; 80 hours of exposure at 80°C produced testpieces which still showed appreciable cohesive fracturing and whose highest failure energies were above those shown on the dry $2\mathscr{T}$ ($\dot{c}$) curve. The toughening effect was now more pronounced while the weakening of the interface is reduced. In other words, $2\mathscr{T}$ has continued to increase while θ has not been significantly reduced. The failure energies observed here were 100% higher than those observed after a comparable exposure to water of pH 7.8.

This result was confirmed by results obtained after 120 hours, 170 hours and 1500 hours exposure to the same environment. Exposure for 120 hours produced results comparable to exposures of 60 hours duration in water of pH 7.8. The positions of the minimum and maximum were essentially unchanged. Failure was completely interfacial after 120 hours exposure.

In an attempt to observe spontaneous separation, a series of testpieces was exposed to this environment for 1500 hours. Spontaneous separation

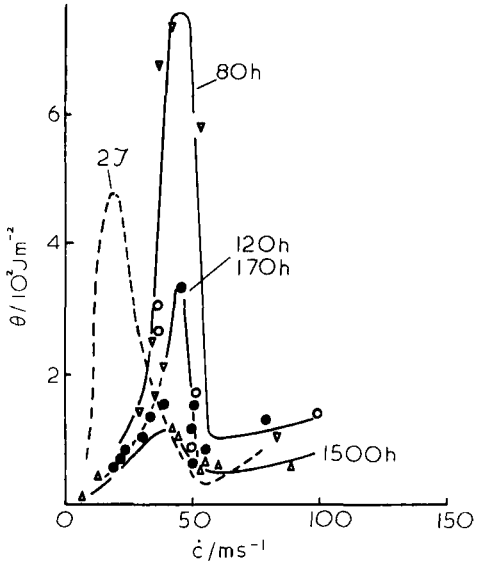

FIGURE 8 As Figure 4, but for pH 8.6.

was not observed, and when tested the samples yielded the data points shown as the bottom curve on Figure 8. This result suggests that there is a tailing off in the weakening effect beyond 120 hours of exposure.

The maximum and minimum of $2\mathscr{T}$ ($\dot{c}$) or θ ($\dot{c}$) occurred at 40 m/s and 60 m/s throughout.

Since the pH of the water bath appeared to have a decisive effect on the fracture behaviour, further investigations were made into the effect of more extremely acid and more extremely alkaline baths.

First, a series of samples were immersed for 120 hours at 80°C in water of pH 13. This environment was obtained by dissolving 5 grams of NaOH pellets in 1 litre of de-ionised water and so contained a high concentration of OH^- ions. After the environmental treatment, the Ti surfaces showed a small amount of tarnishing especially at the sample edges. The mode of failure was completely interfacial with failure energies higher even than those obtained after exposure to water of pH 8.6. The results are shown in Figure 9.

Next, a set of testpieces was subjected to immersion in an acidic bath of water pH 2. This environment was a 0.3% solution of hydrochloric acid in deionised water. The difference in fracture behaviour of these testpieces to that of samples exposed to water of pH 7.8, was small, but significant, as Figure 9 shows. The acid bath caused no visible tarnishing of the titanium surfaces. Immersion in an even more acidic bath of nitric acid, pH 0.1,

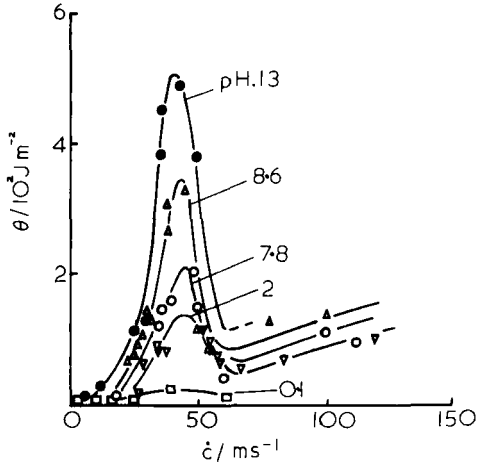

FIGURE 9 As Figure 4, but for 120 h immersion at 80°C and various pH values.

produced an even greater reduction in joint strength, as the lowest curve on Figure 9 shows.

The position of θ_{max} and θ_{min} on the velocity axis is unaltered by the hydrogen ion concentration, occurring again at 40 m/s and 60 m/s respectively. The height of θ_{max} however is considerably influenced by the hydrogen ion concentration of the environmental bath, varying between 510 J/m^2 for pH 13 and 33 J/m^2 for pH 0.1. This relation between θ_{max} and environmental pH is summarised by Figure 10.

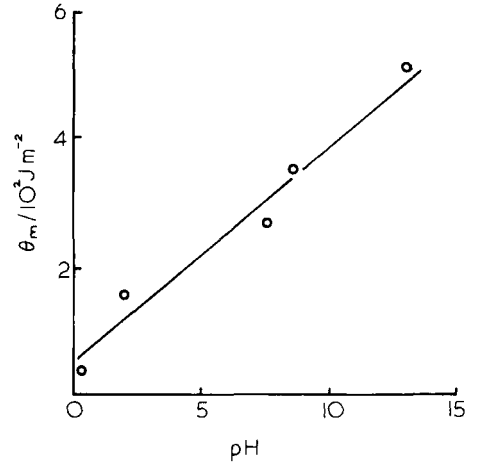

FIGURE 10 Peak values of θ from Figure 9 as a function of water pH.

Effect of water immersion on the bulk mechanical properties of epoxy resins

It is clearly relevant to study the way water immersion changes the bulk mechanical properties of epoxy resin. This was done by testing a series of epoxy cylinders (1 cm dia × 1 cm height) in compression on an Instron testing machine. Both Young's modulus and the yield stress were measured over a range of temperatures and strain rates for testpieces exposed only to air at room temperature and for testpieces exposed to immersion in water (pH 7.0) for 120 hours at 80°C. These conditions were chosen for comparability with the fracture testpieces and are unlikely to produce equilibrium uptake throughout the specimens. The water uptake after such a treatment was 2% by weight. There was also an increase in volume of 1%.

Figure 11 shows a plot of Young's modulus in compression versus test temperature at a medium strain rate of $1.7 \times 10^{-3} s^{-1}$ for both dry and water treated epoxy cylinders. It will be seen that:

1) At temperatures below 60°C, $E_{DRY} > E_{WET}$.
2) For temperatures above 60°C but below T_g, $E_{WET} > E_{DRY}$.
3) The apparent T_g for wet epoxy is shifted to higher temperatures.
4) The modulus changes outlined in (1) and (3) are less than an order of magnitude and typically ~30%

These results suggest that water has a modest plasticising effect on cured epoxy resin, which manifests itself in a lower elastic modulus at low test temperatures, as expected. The fact that $E_{WET} > E_{DRY}$ at higher test temperatures is anomalous, but this result may be understood in terms of additional crosslink formation above T_g. As water diffuses through the matrix during immersion, epoxy molecules begin to enjoy increased mobility and since the immersion temperature is above the T_g of the cured dry epoxy, the increased mobility may give rise to further crosslink formation. It has been shown[2] that an increased crosslink density in epoxy resin is associated with significantly increased T_g and marginally increased Young's modulus. The overall effect of any such increase in crosslink density is thus likely to be a shift of the curve of E against temperature to higher temperatures. At the same time, the wet material is always softer than a dry material of identical T_g because of water plasticisation. The net effect is thus to produce the cross-over observed in Figure 11. The effects of strain rate on E_{DRY} and E_{WET} at a constant test temperature of 25°C is shown in Figure 12, and are similar for both specimen conditions.

The yield stress vs temperature data for wet and dry epoxy also shows a

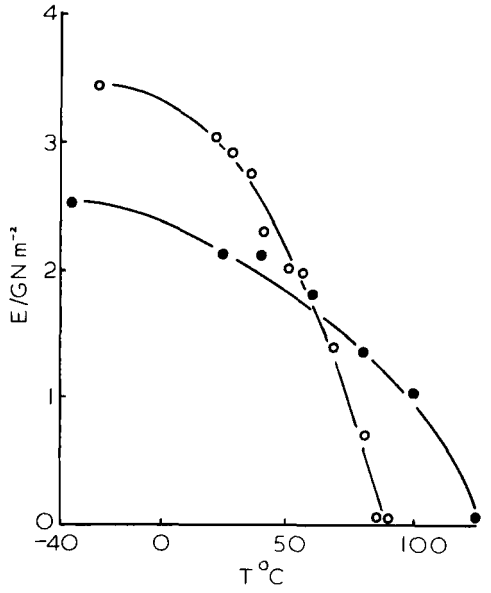

FIGURE 11 Compressive Young's modulus for the epoxy resin at strain rate 1.7×10^{-3} s^{-1} as a function of temperature. (○) dry (●) after immersion at pH 7.0 for 120 h at 80°C.

"crossover" around ambient temperature. (See Figure 13). At low temperatures dry epoxy shows a higher yield stress than wet epoxy while at temperatures above ambient the wet epoxy yield stress, σ_y, is higher than the dry epoxy yield stress. These results are to be expected from the plasticisation and postcuring mechanism proposed in the preceeding paragraph. The effects of strain rate on yield stress at 25°C are shown in Figure 14.

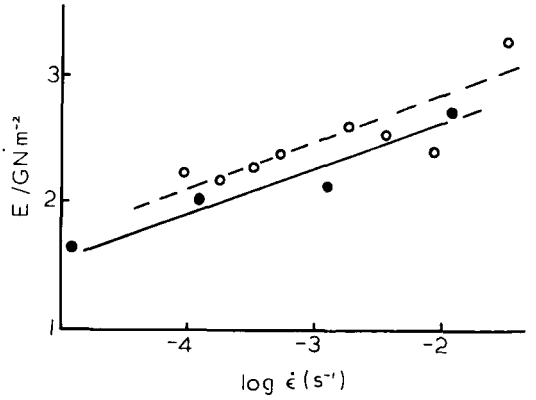

FIGURE 12 As Figure 11 but as a function of strain rate at 25°C.

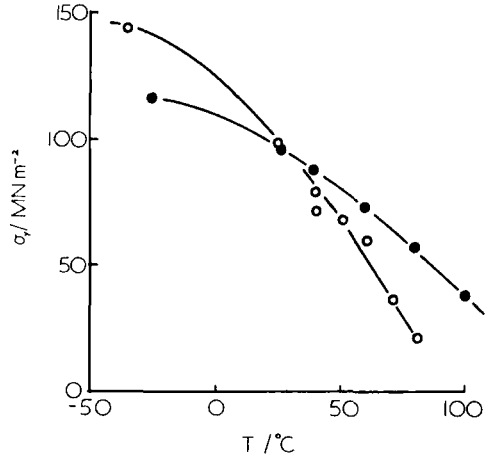

FIGURE 13 Compressive yield stress for the epoxy resin as a function of temperature at strain rate 1.7×10^{-3} s^{-1}. (○) dry (●) after immersion at pH 7.0 for 120 h at 80°.

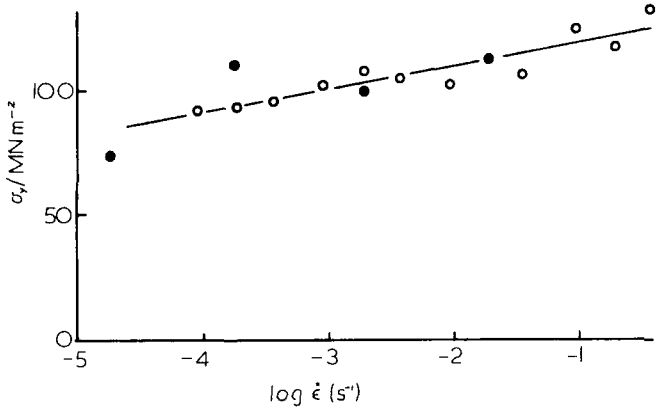

FIGURE 14 As Figure 13 but as a function of strain rate at 25°C.

DISCUSSION

Summary of findings

In this and previous papers,[1,5,6] the cohesive and adhesive fracture strengths of epoxy resin systems have been characterised in terms of fracture energy plotted as a function of crack velocity. The particular epoxy resin employed in these studies, when tested below T_g, always exhibits a strong dependence of fracture energy upon crack speed, with a sharp maximum at a velocity below 50 m/s. This general pattern of behaviour has now been observed for cohesive fracture of sheet specimens of the resin,[12] adhesive failure of epoxy

to metal bonds having a sheet configuration[5] plane strain cohesive fracture,[1] plane strain adhesive failure of epoxy to metal bonds and, as reported in this paper, plane strain adhesive failure of environmentally degraded adhesive bonds.

Differences are induced in the curve of fracture energy versus $\dot{c}$ by changes in the state of stress around the pre-formed crack. Such changes occur, for example, as we move from the plane strain test configuration employed in the present paper and in reference,[1] to a sheet specimen which exhibits mixed plane-strain/plane stress conditions. Further modifications of the stress field arise in the plane-strain specimens according to whether the pre-formed crack is located in the bulk of the compliant phase (epoxy resin) or at its interface with a relatively rigid metal substrate. These changes will be discussed in a separate paper, together with the reasons for the extreme rate sensitivity displayed by both cohesive and adhesive fracture energies.

The purpose of this paper is to examine the changes in adhesive failure energy of epoxy-titanium joints induced by environmental ageing in aqueous media. These changes can be summarised as follows.

a) The original dry specimens fracture cohesively through the epoxy resin even though the pre-formed crack is located at the adhesive interface. The curve of $2\mathcal{T}$ versus $\dot{c}$ rises to about 500 J/m^2 at a crack velocity of 20 m/s. (When the pre-formed crack is located in the bulk of the epoxy resin the peak fracture energy occurs at 37 m/s). The data are the same for a variety of metal substrates (Au, Ti, brass). There is a suggestion of a minimum in the curve at around 60 m/s.

b) Immersion times in water of up to 30 h at 80°C produce no change in the fracture energy vs $\dot{c}$ curve, although a progressive increase is observed in the proportion of the fracture surface which is adhesive (interfacial) rather than cohesive.

c) At longer immersion times (>60 h) and even at temperatures as low as 20°C, the peak in the curve shifts to higher $\dot{c}$ values in the range 40–50°C. At the same time the peak fracture energy may increase significantly if the environmental fluid has a sufficiently alkaline pH.

d) All subsequent exposure to the environmental fluid produces progressive deterioration in fracture energy without significant changes in the shape or position of the curve. The deterioration is most rapid at higher temperatures (especially above T_g of the resin), and, more surprisingly, at low environmental pH.

e) No exposure conditions were found in the present work at which the joint was so weakened as to separate spontaneously. No gross chemical

changes occurred at the bonded metal surface with Ti, unlike the extensive oxidation found with mild steel substrates,[13] though some tarnishing of the Ti was observed.

Plasticization

It is well known that epoxy resins can absorb significant amounts of water and that the absorbed water can modify the mechanical properties of the materials. In particular we have found a decrease in yield strength at test temperatures below about 30°C. It is most likely, therefore, that the shift in the peak of the fracture energy curve to higher $\dot{c}$, together with the elevation of fracture energy observed in some environments, is caused by water plasticisation affecting the relaxation time spectrum of the epoxy resin, and thence the loss function Φ (see later).

It is not possible at present to provide a more quantitative account of the plasticisation effects, since the mechanism controlling fracture energy in the dry system is not yet understood except in broad qualitative terms. One interesting feature, however, is that once the peak in the fracture energy curve has shifted to about 40 m/s, no significant further shift occurs even after prolonged immersion. This suggests that equilibrium water uptake is achieved after no more than 120 h at 20°C and 60 h at 80°C. This may not mean that the resin is saturated throughout its volume after these times, but merely that the initiation region around the flaw tip has achieved equilibrium.

At first sight it may appear that the water pH has an effect in controlling the level of plasticisation. This is because the peak value of fracture energy is enhanced far more at high pH than at low pH. Against this, however, the position of the peak on the $\dot{c}$ axis is unaffected by the environmental pH, and, as we shall see presently, the loss function Φ appears independent of pH. The most likely explanation of the peak values is that the increase in $2\mathscr{T}$ due to plasticisation is offset by the decrease due to interfacial weakening. At high pH the latter effect is minimised so that much more of the potential toughening due to plasticisation is realised under these conditions. We believe, therefore, that plasticisation is unaffected by the pH of the environment.

Diffusion and the locus of failure

As we have already seen, the variation in the locus of failure with increasing time and temperature of immersion, can be explained by a diffusion process. A critical concentration of water at the interface is achieved which reduces the interfacial bond strength below the cohesive strength of the resin resulting in failure at or close to the interface over the relevant regions of the bond. The achievement of interfacial separation does not immediately, however, reduce the fracture energy values.

These observations can be rationalised in terms of Andrews' fracture Eq.[3]

$$\left.\begin{aligned} 2\mathscr{T} &= 2\mathscr{T}_0\Phi(\dot{c}, T) \text{ cohesive bond failure} \\ \theta &= \theta_0\Phi(\dot{c}, T) \text{ adhesive bond failure} \end{aligned}\right\} \quad (8)$$

where Φ is the loss function and $2\mathscr{T}_0$, θ_0 are the energies required to break unit area of interatomic bonds across the fracture plane for, respectively, the cohesive and adhesive cases.

The critical water concentration referred to above can thus be portrayed as that concentration required to reduce θ_0 from a value significantly higher than $2\mathscr{T}_0$ to a value just lower than $2\mathscr{T}_0$. This would result in an immediate change of locus from cohesive to interfacial without a dramatic change in $2\mathscr{T}$ or θ.

As the interfacial water concentration builds up beyond the critical value and (possibly more important) with the increasing passage of time, the interfacial bonding is progressively weakened *i.e.* θ_0 decreases with time, without change of Φ which is determined wholly by the properties of the now-plasticized resin.

The loss of function Φ

In order to test the applicability of Eq. (8), we propose the following model of the processes under investigation.

Let Φ_1, $\mathscr{T}_{01}$, θ_{01} be the relevant parameters for the dry specimens and $\Phi_2, \mathscr{T}_{02}, \theta_{02}$ for specimens subject to environmental ageing. We have already suggested that plasticisation results in the change $\Phi_1 \rightarrow \Phi_2$ and that once this change has occurred, Φ_2 remains invariant with time. We further assume that $\mathscr{T}_{01} \simeq \mathscr{T}_{02}$, *i.e.* that the cohesive bond fracture energy is not affected significantly by plasticisation. Finally we suppose that θ_0 is reduced progressively with time by the arrival and reaction of water molecules or ions at the interface.

The predictions of the model are testable in two respects. Firstly we predict an abrupt change of fracture locus at the point where θ_{02} first decreases below $2\mathscr{T}_{02}$, *without* a corresponding abrupt change in $2\mathscr{T}$ or θ. This is observed as already mentioned. Secondly, by taking logarithms we find,

$$\log \theta_2 = \log \theta_0 + \log \Phi_2(\dot{c}, T) \quad (9)$$

and if $\log \theta_2$ is plotted again $\dot{c}$ (or $\log \dot{c}$) the resulting curves should be superimposable by a vertical shift, whatever the environmental history, provided only that the condition $\Phi = \Phi_2$ has been established.

In Figure 15 are plotted all data obtained for exposure at 80°C, in the form,

$$(\log \theta_2 + \log \alpha_i) \text{ versus } \log \dot{c} \quad (10)$$

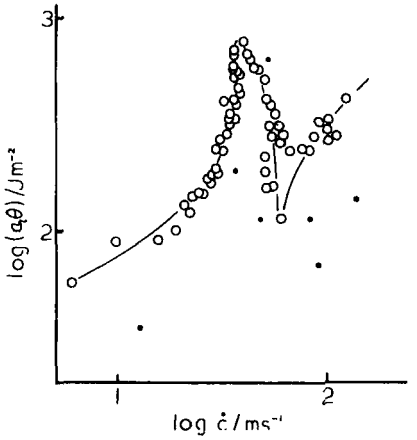

FIGURE 15 Master curve of log $\alpha_i\,\theta$ versus log (crack velocity) obtained by vertical shifts of log θ *vs* log $\dot{c}$ curves. All data from 80°C immersion tests but covering different times of immersion and pH conditions. Black dots are "stray" points indicating magnitude and incidence of experimental scatter.

where log α_i are the vertical shifts required to give the best superposition of data obtained at different times and pH values. It will be seen that a high degree of superposition can be obtained, especially to the left of the peak. The more scattered data to the right of the peak, together with "stray" points indicated by small dots, can reasonably be attributed to experimental scatter (see Ref. 1).

The process has been repeated in Figure 16 for data relating to exposure

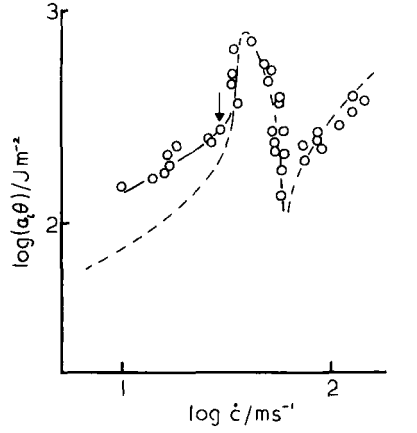

FIGURE 16 As Figure 15 but for all data obtained at temperatures below 80°C. Broken curve represents the data of Figure 15. Arrow indicates position of peak in curve for unimmersed specimens.

temperatures below 80°C (*i.e.* the data of Figure 6). The broken line is the master curve from the previous Figure. Once again good superposition is obtained except for the region below about 20 m/s which corresponds to the peak in Φ_1, *i.e.* the loss function for the unplasticised resin. It seems quite clear that at these lower temperatures there is residual memory of the unplasticised rheological behaviour even though the "plasticised" peak at 40 m/s is well developed.

The shift factors and θ_0

Comparison of Eq. (9) and (10) shows of course that,

$$\log \alpha = - \log (a\theta_{02}) \tag{11}$$

where a is an arbitrary constant. The shift factors can therefore be used to determine the relative changes of θ_{02} with time, temperature and pH value in the environment.

These changes are such as to fit the following model. In what follows θ_{02} is written θ_0 for brevity.

Suppose that the dry interface consists of a single species, A, of interatomic bond of dissociation energy U_A, with N bonds/unit area. The bonds A can be hydrolysed by H^+ ions to a form B having a lower dissociation energy U_B having a lower dissociation energy U_B, and hydrolysis proceeds at a constant rate designated by a rate constant k, which will be a function of the H^+ concentration. Then,

$$\left.\begin{aligned} \theta_0(t) &= nU_A + (N-n)U_B \\ \theta_0(0) &= NU_A \\ \theta_0(\infty) &= NU_B \end{aligned}\right\} \tag{12}$$

where t is the time and n is the number of bonds A intact at any time. Then

$$\begin{aligned} \frac{d\theta_0}{dt} &= (U_A - U_B)\frac{dn}{dt} = -kn(U_A - U_B) \\ \theta_0 &= N(U_A - U_B)e^{-kt} + NU_B \\ \theta_0 &= \{\theta_0(0) - \theta_0(\infty)\}e^{-kt} + \theta_0(\infty) \end{aligned} \tag{13}$$

or,

$$\ln \left\{ \frac{a\theta_0 - a\theta_0(\infty)}{a\theta_0(0) - a\theta_0(\infty)} \right\} = -kt \tag{14}$$

where the arbitrary constant a has been introduced.

Equation (14) is used to obtain k values for data at pH values of 7.8 and 8.6 at 80°C. (Figure 17). Using these data, Figure 18 has then been plotted in the form of Eq. (13), *i.e.* $a\theta_0$ versus $\exp(-kt)$ using the appropriate values of k.

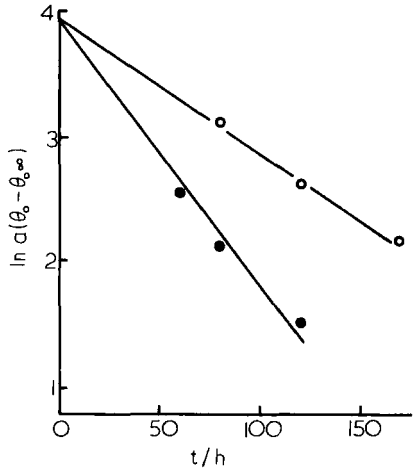

FIGURE 17 Logarithmic plot of θ_0 versus time, demonstrating first-order reaction kinetics of the acid-catalysed hydrolysis of interfacial bonds. (○) at pH 8.7 (●) at pH 7.8. Temperature of immersion 80°C.

A single straight line is obtained with a slope

$$a\{\theta_0(0)-\theta_0(\infty)\} = 55 \text{ J/m}^2$$

If it is assumed that $\theta_0(1500 \text{ h})$ is approximately equal to $\theta_0(\infty)$, as Figure 18 would suggest, we obtain

$$a\theta_0(0) = 62 \text{ J/m}^2$$
$$a\theta_0(\infty) = 7 \text{ J/m}^2$$

The question now arises as to whether it is possible to obtain absolute values for θ_0 by finding a value for the arbitrary constant a. The data reported in this paper certainly do not permit this, but an estimate for a can be obtained by the following reasoning.

Theoretical and experimental values of $2\mathscr{T}_0$ have been obtained for the epoxy resin employed in these tests from experiments carried out above T_g.[6] This value was,

$$2\mathscr{T}_0 = 2.59 \text{ J/m}^2$$

At $t = 0$ fracture is still cohesive in the present tests, indicating that $\theta_0 > 2\mathscr{T}_0$. The transition to adhesive failure occurs (for 80°C and pH 7.8) in the time interval 30 h $< t <$ 60 h and at this change-over we may assume $\theta_0 \sim 2\mathscr{T}_0$. Referring to Figure 18 we find that this time interval corresponds to an interval

$$20 < a\theta_0 < 35 \text{ J/m}^2$$

Taking an average value of $a\theta_0 \simeq 27 \text{ J/m}^2$ and equating it to $2\mathscr{T}_0$ we

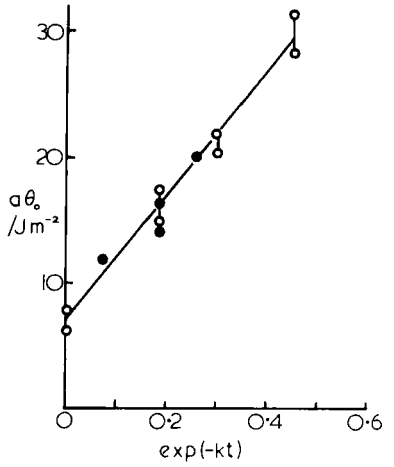

FIGURE 18 Composite plot of $a\theta_0$ against exp $(-kt)$ using appropriate k values from Figure 17 (○) at pH 8.7 (●) at pH 7.8.

obtain a $\simeq 10$ and

$$\theta_0(0) \simeq 6.2 \text{ J/m}^2$$
$$\theta_0(\infty) \simeq 0.7 \text{ J/m}^2$$

It is interesting to compare these figures with those obtained for the same resin bonded to steel, Al and gold surfaces by Andrews and King.[5] They found, for dry joints against all three metals,

$$0.6 < \theta_0 < 0.8 \text{ J/m}^2$$

and also showed that these values were, at the most, only a factor of two greater than the thermodynamic works of adhesion, *i.e.* the bond was almost certainly due to secondary interatomic interactions.

In the present work it appears that the initial dry joint is some ten times stronger than obtained on steel, Al and gold, and this harmonises with the fact that the failure locus was interfacial for these three metals but cohesive for Ti. In the work of Andrews and King, an epoxy resin of *different* composition was found to give $\theta_0 \sim 8$ J/m^2 when bonded to stainless steel, and this was attributed to the formation of primary, ether-type linkages between epoxide groups and iron oxide. The results for dry titanium bonds may be explicable in the same way.

After prolonged exposure to water, θ_0 falls to an apparently steady value of around 0.7 J/m^2, *i.e.* very close to the θ_0 values obtained for dry joints with other metal substrates and to the thermodynamic work of adhesion for these systems. It is tempting therefore to conclude that the residual strength of the epoxy–Ti bond after environmental exposure is due to van der Waals interactions after hydrolysis of the primary bonds.

This, however, may be a naïve interpretation. For one thing, water would be expected to displace secondarily-bonded resin completely from a high energy surface,[11,13] leaving a residual strength no greater than $\theta_0 = 2\gamma$ where γ is the surface energy of water. This is five times smaller than the $\theta_0(\infty)$ actually observed. It is more likely, therefore that the residual strength results from a limited number of permanent primary bonds at the interface, perhaps of a non-hydrolysable species.

The hydrolysis reaction itself is clearly faster in acid environments and this provides a pointer to the chemistry of the process. The most likely mechanism is the acid catalysed cleavage of ether linkages, between the resin and the oxide surface, by a carbonium ion process.[14] This matter is still under investigation and will be reported on in a future paper.

References

1. E. H. Andrews and A. Stevenson, *J. Mater. Sci.* **13,** 1680 (1978).
2. A. Stevenson, Ph.D. Thesis, *Cohesive and Adhesive Failure of Epoxy Resin Systems.* (Univ. of London), 1978.
3. E. H. Andrews, *J. Mater. Sci*, **9,** 887 (1974).
4. E. H. Andrews and A. J. Kinloch, *J. Polymer Sci.* **C46** 1 (1974).
5. E. H. Andrews and N. E. King, *J. Mater. Sci.* **11** 2004 (1976).
6. N. E. King and E. H. Andrews, *J. Mater. Sci.* **13** 1291 (1978).
7. A. Peterlin, *Makromol. Chem.* **124** 136 (1969).
8. H. L. Frisch, T. T. Wang and T. K. Kwei, *J. Polymer Sci.* **A2,** 7 879 and 2019 (1969).
9. R. A. Gledhill, A. J. Kinloch and S. J. Shaw, *J. Adhesion* (to be published).
10. J. Manson and E. Chui, *J. Polymer Sci.* **C41** 95 (1973).
11. R. Gledhill and A. Kinloch, *J. Adhesion* **6** 315 (1974).
12. E. H. Andrews and N. E. King, *Polymer Surfaces* ed. D. T. Clark and W. J. Feast (J. Wiley and Sons, New York, 1978) p. 47.
13. R. Gledhill and A. J. Kinloch *Weathering of Plastics and Rubbers* (Plastics and Rubber Institute, London, 1976) paper D12.
14. E. R. Alexander, *Principles of Ionic Organic Reactions* (J. Wiley and Sons, New York; Chapman and Hall, London), p. 218.
15. J. Crank, *Mathematics of Diffusion* 2nd Ed. (Oxford Univ. Press, 1956), equation 2.45.